Cote d'ivoire

N° : 827

INTERNATIONAL MASTER PROGRAM

IN RENEWABLE ENERGY AND GREEN HYDROGEN

SPECIALITY: Green Hydrogen Production and Technology

MASTER THESIS

Subject/Topic:

Microstructural Characterization and Study of Hydrogen Embrittlement in Austenitic and Ferritic Stainless Steels

Presented On the

23rd September 2025

and by:

Ibrahim Modu Aji

Professor KOUADIO Kouassi Yves	**President of the jury**
Professor ESSI Marc Marie-Maurice Mélège	**Examiner**
Dr TILLOUS Kessein Eric	**Main supervisor**
Prof. Dr.-Ing. Ulrich Krupp	**Co-Supervisor**

Academic year 2024-2025

DEDICATION

I dedicate this research work to my dearest Mother, **Kellu Modu Aji**, her love, prayers and encouragement have been my cornerstone of my journey and for my late Father, **Modu Aji Tijjani**, whose values and guidance continue guide what I do.

I also dedicate this dissertation to my elder sister **Yanagana Modu Aji** and my younger brothers **Ismail Modu Aji** and **Muhammad Modu Aji** whom have supported me throughout the process. I will always appreciate all their constant encouragement, especially Yanagana.

ACKNOWLEDGEMENTS

First and foremost, I express my profound gratitude to the West African Science Service Centre on Climate Change and Adapted Land Use (WASCAL) for granting me the scholarship that made my studies possible. Without this generous support, my academic journey and the realization of this research would not have been possible.

My heartfelt appreciation goes to the President of, for granting me admission and support during the first and second semesters of the International Master Program in Renewable Energy and Green Hydrogen. I am equally grateful to the President of Félix Houphouët-Boigny University for the final approval and for granting the certificate that crowns this effort.

I sincerely thank the of rector of RWTH Aachen University Prof. Ulrich Rüdiger, where I had the opportunity to complete my internship in Germany. The experience gained during that period has been invaluable in shaping my research and professional outlook.

I acknowledge with deep gratitude the support of the Director Prof Adamou Rabani of the Graduate Studies Program (GSP) at Abdou Moumouni University, and Director of the GSP at Félix Houphouët-Boigny University where I will obtain my certificate. My thanks also go to the Deputy Director of the GSP for guidance and administrative support.

I wish to extend my appreciation to the Coordinator of the Hydrogen (H_2) Programme Dr. Fassinou Wanignon, whose leadership has ensured the success of this program, and to the Scientific Coordinator for his/her academic guidance and constructive feedback throughout the course of study.

Special thanks go to my Major Supervisor, Prof. Ulrich Krupp and Dr. Kessein Tillous, for their invaluable guidance, mentorship, and encouragement during the research process. I am equally grateful to my Co-Supervisor, Nima Babaei, M.Sc., for his continuous support, insightful suggestions, and constructive criticism that shaped this work.

I respectfully acknowledge the evaluation of Professor KOUADIO Kouassi Yves (President) and Professor ESSI Marc Marie-Maurice Mélège (Examiner). While I am disappointed of their unfairly grading that did not fully reflect the depth of my effort, I remain appreciative of the critiques that encourage further improvement.

My sincere appreciation once again goes to Prof. Ulrich Krupp, the Director of Steel Institute at RWTH Aachen University, for hosting me during my internship and providing me with the facilities and professional support that enriched this research.

I would also like to recognize the contributions of the team members from Niger who supported me during the first and second semesters. Their collaboration and solidarity made my academic journey more fulfilling.

Finally, to my friends, colleagues, and all others who directly or indirectly supported me during this journey, I am grateful. Your encouragement and kindness will always be remembered.

Above all, I thank Almighty God for the strength, guidance, and perseverance granted to me throughout this Endeavor.

ABSTRACT

Hydrogen Embrittlement is a vital materials degradation phenomenon in stainless steels, leading to materials premature failure and decreased ductility in hydrogen-rich conditions. Duplex stainless steels (DSSs), with their special characteristics coming from dual-phase of ferritic-austenitic structure of roughly equal parts (50%-50%), containing a mixture of high rich elements such as chromium, molybdenum and nitrogen are widely used in chemical and energy industries because of their strength and corrosion resistance. Despite their long- standing reliability Duplex stainless steels (DSSs) in hydrogen rich-environments is one the most concern issue especially as interests in hydrogen technologies kept growing towards sustainable energy transitions.

This research work seeks to study the chemical compositions and microstructures of the duplex stainless steel, evaluate the mechanical properties and determine the hydrogen content and trap distributions to see how the effects of phase balance on the mechanical properties of the duplex stainless steel. To achieve these, electrochemical hydrogen charging, slow strain rate tensile (SSRT), thermal desorption Analysis (TDA) and scanning electron microscopy (SEM) fractography was performed.

The finding shows that the unaffected by hydrogen parameter is yield strength while on the other hands, time considerably decreased under hydrogen charging for tensile strength, elongation and fracture time. According to the thermal desorption analysis (TDA) measurement conducted, hydrogen uptake was confirmed with release curves dominated by peaks in the mid-range temperatures, indicative of characteristic trapping sites. The fractographic results under SEM revealed that uncharged samples exhibit a ductile fracture characterized by uniform dimples in the uncharged, while hydrogen-charged samples exhibit a ductile-brittle mixture with both ductile dimples and brittle microcracks. These findings demonstrate that hydrogen ingress promotes embrittlement through ductility loss and altering of the fracture modes.

ACRONYMS AND ABBREVIATIONS

FCC : Face-Centred Cubic

BCC : Body-Centred Cubic

DSS : Duplex Stainless Steel

HE : Hydrogen Embrittlement

HEDE : Hydrogen-Enhanced Decohesion

HELP : Hydrogen-Enhanced Localized Plasticity

SSRT : Slow Strain Rate Testing

TDA : Thermal Desorption Analysis

TDS : Thermal Desorption Spectroscopy

UNS : Unified Numbering System (for alloys)

SSC: Stress Corrosion Resistance

EN: European Union

WASCAL : West African Science Service Centre on Climate Change and Adapted Land Use

LIST OF TABLES

LIST OF FIGURES

Table of Contents

Introduction

In the quest to attain clean energy solutions and mitigate climate change, hydrogen is fast becoming a recognised key player as a carrier for clean energy owing to its zero-carbon emission and high energy density at the points of application. A major challenge, however, depends on mitigating materials degradation and hydrogen embrittlement for safe and efficient use of hydrogen. Duplex stainless steel constitutes an integral storage system, pipelines, and modern energy applications. Therefore, investigating hydrogen compatibility and microstructure is essential for a safe, dependable, and decarbonized energy system.

Duplex stainless steels (DSSs) a group of stainless steels characterized by their approximately equal proportions of ferrite and austenite. They possess a mixture of the most beneficial of both austenite and ferrite stainless steel. This combination of characteristics translates into high mechanical strength and stress corrosion cracking, leading to their applications in the oil, gas and chemical industries (Nilsson, 1992). Despite their exceptional mixture of characteristics of both strength and corrosion resistance, the two phases of the DSSs also make them vulnerable to hydrogen embrittlement. This is because hydrogen can interact differently with the austenite and ferrite phases, which can degrade performance in hydrogen-rich environments. Hydrogen embrittlement (HE) is a serious material degradation that affects steels and other alloys when they are subjected to hydrogen-rich environments. This results in a substantial compromise of the ductility of the material and toughness, resulting in abrupt and extensive failures (Javeria & Kim, 2025). The importance of understanding hydrogen embrittlement is necessary for ensuring a reliable and safe applications in different sectors such as petroleum, energy and structural usage. The growing considerations of the vital of duplex stainless steel in terms of hydrogen storage related technology, an investigation into the susceptibility of the materials is essential. In this context, this research work raises an important question. First, under different heat treatments, how does microstructure and chemical compositions of the DSSs response? Second, using SSRT, with and without hydrogen how does do the mechanical properties of sample respond? Third, Quantity of the hydrogen content and distribution of the trap within the sample and lastly, in terms of the phase balance, how does it influence the technological and mechanical properties of the DSSs?

These questions underscore the critical knowledge gap that this thesis aims to address. Therefore, this has further led to formulate the objective as to characterize the effects of hydrogen on the mechanical behaviour, microstructure, and fracture mechanisms of duplex stainless steels. the specific objectives as sentences:

1. To analyse the chemical composition and microstructure of duplex stainless steels subjected to different heat treatments.
2. To evaluate mechanical properties using slow strain rate testing (SSRT) with and without hydrogen charging.
3. To determine the hydrogen content and trap distribution using thermal desorption analysis (TDA).
4. To investigate the effect of phase balance on the mechanical-technological properties of duplex stainless steels.

CHAPTER 1: LITERATURE REVIEW

1.1 Duplex Stainless Steels: An Overview

Duplex alloys represent the newest fast-growing family of stainless steels. Duplex stainless steel (DSSs) is a mixture of microstructures of ferrite and austenite in almost equal proportions that has been in existence for over 70 years. The ferritic-austenitic grades have a ferrite matrix intermixed with austenite, an island of austenite in a continuous matrix of highly alloyed ferrite, commonly called "Duplex" stainless steel. Duplex stainless-steel covers ferritic/austenitic Fe-Cr-Ni alloy between 30% to 70 % Ferrite. Due to the high level of Cr, Mo, and N, steels show high pitting & stress corrosion cracking resistance in chloride-containing environments. Hence, it is frequently used in oil refinery heat exchangers & typical applications where there is a risk for SCC and localized corrosion because of chloride-containing process streams, cooling waters or deposits. Modern duplex stainless steels have generally good weldability (Kahar, 2017).

Duplex stainless steels contain more than 19 wt.% Cr and have more than 30 wt.% of both ferrite and austenite (Francis & Byrne, 2021). Modern duplex stainless steels contain approximately 50/50 austenite and ferrite in their microstructure, and they combine the high strength of ferrite with the ductility and toughness of the austenite. The addition of nitrogen enables better equi-partitioning of elements between the two phases, higher strength in the austenite, better corrosion resistance, and improved weldability, to name but a few benefits (Lizlovs, 1981; Foct, Magnin, Perrot, Vogt,1991).

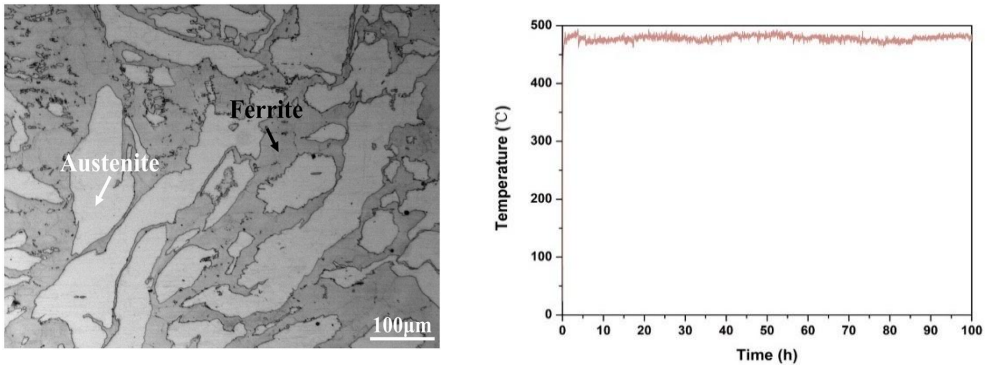

(a) **(b)**

Figure 1: (a) Microstructure of DSSs (b) Temperature evolution of the sample (Liu et al., 2022).

The typical microstructure of the duplex stainless steel after solution treatment at 1050 ˚C for 1 h and quenching is shown in Fig 1 (a), which is composed of the ferrite phase in dark contrast and austenite phase in a light grey contrast. The fraction of ferrite and austenite is approximately 1:1 measured by Ferrite Scope (Fischer Periscope MP30). The isothermal aging treatment of the duplex stainless steel is performed at 475 ˚C for 60 h and 100 h, respectively, and the temperature fluctuation range of the muffle furnace is ±5 ˚C. The parameters of pulsed electric field are adjusted to hold the sample temperature at 470– 480 ˚C, and the parameters are 150 Hz-150 μs-190A. The pulsed sample with 30 × 5 × 0.5 mm^3 is fixed on the designed mold with a K-type thermocouple to record the resulting temperature, and the resulting temperature is displayed in Fig 1(b) (Liu et al., 2022).

1.2 Roles and Functional Importance of Duplex Stainless Steels

It is well known that the duplex stainless steels (DSSs) possess high strength and excellent corrosion resistance, with relatively low cost. So, they are increasingly used as structure materials in many applications, such as offshore platforms, oil and gas production, chemical plants, pulp and paper industries, nuclear reactors, and process systems, where both high mechanical strength and high corrosive resistance are required (Duplex Stainless Steels, n.d.; Nilsson, 1992). Studies have shown that they have better resistance to stress corrosion cracking (SSC), crevice and better pitting corrosion, especially efficient in chloride-rich environments due to the presence of optimized alloying elements like Cr, Mo, and N (Liou et al., 2001; Paulraj & Garg, 2015). An approximation of the dual-phase structure of ferrite and austenite (commonly 50-50) improves their functional performance by bringing together the strength of ferrite with corrosion resistance of austenite (Łabanowski et al., 2014; Liou et al., 2001)

Duplex grades contain high Cr, high N and low Ni contents with increased mechanical properties (yield strengths twice the value of austenitic grades (Boillot & Peultier, 2014). It has been widely acknowledged that the competitivity of DSSs is increasingly rising considering the market demand of high-quality corrosion-resistant materials, the advancement of manufacturing technologies and the raw material pressure of nickel which has been a major element in austenite stainless steels (ASSs) (Zhang et al., 2022)

DSSs have attracted more attentions for structures in corrosive environment such as ship building, marine engineering, chemical engineering, paper, pulp and petrochemical industries (Chemelle, 2011).

1.3 Alloying Elements in Duplex Stainless Steels and Their Functional Roles

The most important alloying elements in DSSs are C, Cr, Ni, Mn, N, and Mo, which directly affect the microstructure and properties of the steels. Meanwhile, other alloying elements such as Cu, W, and rare earth also play a key role in the performance of DSSs (Han et al., 2023).

It is known that Cr and Mo are ferrite formers and Ni, and N are austenite stabilizers. It has long been recognized that Cr is the major element used to form the passive film, which improves the localized corrosion resistance and oxidation resistance (Łabanowski et al., 2014). The role of Mo is found to cause increases in the stability of the passive film, the pitting and crevice corrosion resistances (Adhe et al., 1996).

Nitrogen can greatly improve the passivation property of the stainless steel, especially the resistance to pitting and stress corrosion in chloride environments (Chou et al., 1997; Nilsson, 1992). It has been established that N alloying enhances the protective characteristics of the passivation film by creating an N-enriched layer at the interfacial region between the metal and the passivation film (Chou et al., 1997; Ha et al., 2012; Levey & van Bennekom, 1995a).

1.4 Typical Composition Ranges of Duplex Stainless Steels

Traditional DSSs usually contain 18–26Cr, 3–8Ni, 2–5Mo, and 1–2Mn (in wt.%) [6, 8–11], and the proportion of any constituted phase is more than 30%. For example, for super and hyper duplex stainless steels (S(H)DSSs), in addition to high contents of Cr, Ni, Mo, and N, W and Cu are commonly added. The increased degree of alloying results in the pitting corrosion resistance equivalent value (PRENT) greater than 40. The addition of these alloying elements leads to property improvements that can be traced to a large degree on their effect on phase transformations (Gouné et al., 2015).

Duplex stainless steel encompasses a wide array of compositions and corrosion resistance levels and are typically divided into four categories: lean, standard, super and hyper duplex. Lean duplex stainless steels such as 2304, 2101, 2102, and 2202 are characterized by less

nickel and molybdenum. They have PREN values within the range of 24-30, providing corrosion resistance close to 316L stainless steel while being greater in strength and affordable. Standard duplex (namely 2205, PREN ~35) and super duplex steels (like 2507, PREN >41) exhibit enhanced corrosion resistance owing to their higher Cr, Mo, and N content. Super duplex grades can outperform 6 wt.% Mo austenitic, with advantage steels at a lower cost due to reduced nickel content. Hyper duplex grades (such as 2707, with PREN around ~49) exhibit high Cr (27-32%) and N (0.4-0.5%) levels, resulting in outstanding pitting resistance, but are difficult to process due to the formation of an intermetallic phase during process limiting them to thin-walled products (Francis & Byrne, 2021).

Table I: Typical compositional ranges of DSSs and their properties (Francis & Byrne, 2021)(Francis & Byrne, 2021).

Category	**Example alloys (UNS. No)**	**Key Alloying elements (wt.%)**	**PREN Range**	**Corrosion Resistance Level**
Lean Duplex	S32304, S321O1	Cr:20-23% Ni:1.5-5% Mo:0.3-1.9% N:1.0-0.22%	24-30	Equivalent in properties to 316L austenitic stainless steel.
Standard Duplex	S32205, S31803	Cr:22% Ni:5% Mo:3-3.2% N:0.1-0.22%	34-36	Superior resistance to stress corrosion cracking (SSC) than 316L.
Super Duplex	S32750, S32760	Cr:25% Ni:7% Mo:3.5-4% N:0.24-0.32%	≥ 40	Performs similar functions to 6 Mo austenitic stainless steel.
Hyper Duplex	S32707, S33207	Cr:27-32% Ni:6.5-7% Mo:4.8-5% N:0.4-0.5%	≥ 48	Outstanding performance to pitting resistance.

1.5 Influence of Alloying Elements on Ferrite–Austenite Phase Stabilities

Chromium is a typical ferrite-forming element. In DSS, Cr is the most essential and decisive element, which can expand the ferrite phase region and stabilize the ferrite structure (Lee, 2006; Park, 2002; Ravindranath & Malhotra, 1995). Cr can form a dense oxide protective

film on the surface of stainless steel, improving the repair and repassivation abilities of the damaged passivation film (Han et al., 2023).

Nitrogen is known to be strong austenite stabilizing element and is equivalent to 30 times that of nickel in stabilizing austenite (Li et al., 2011). Generally, N exists in austenite as an interstitial solid solution, which can improve the strength of austenite (Levey & van Bennekom, 1995b). In the DSSs, the N content in the austenite determines the relative mechanical properties of the constituent phases to some extent (Choi et al., 2012; Fujisawa et al., 2014; Moverare & Odé, n.d.; Papula et al., 2016). The addition of N also aggregates Cr and Mo in the austenite, reducing the Cr and Mo concentrations required for the growth of the σ phase in the ferrite and reducing the activity of Cr and Mo (Kim et al., n.d.; Newman & Shahrabi, 1987; Palit et al., 1993).

Table II: Alloying elements in stabilizing ferrite-austenite phases in DSSs (Kim et al., n.d.; Newman & Shahrabi, 1987; Palit et al., 1993)

Element	**Stabilizing effect**	**Functional effect**	**Phase control impact**
Cr	Ferrite forming	Corrosion resistance Strength	Expands ferrite region
Mo	Ferrite forming	Pitting resistance	Stabilizes ferrite
Ni	Austenitic forming	Ductility Austenite stability	Promote Austenite Formation
N	Strong Austenite	Pitting resistance Austenite stability	Strongly Stabilizes austenite

1.6 Hydrogen Embrittlement Mechanism

Hydrogen present in high strength material namely steels have a widely common influence known as hydrogen embrittlement. It is defined as the process by which strength of a material can reduced significantly by introduction of hydrogen atom when working on hydrogen environment. Simultaneously ductility of a material is reduced and make it brittle. This

occurs in many metals including steels, nickel (Dwivedi & Vishwakarma, 2018).

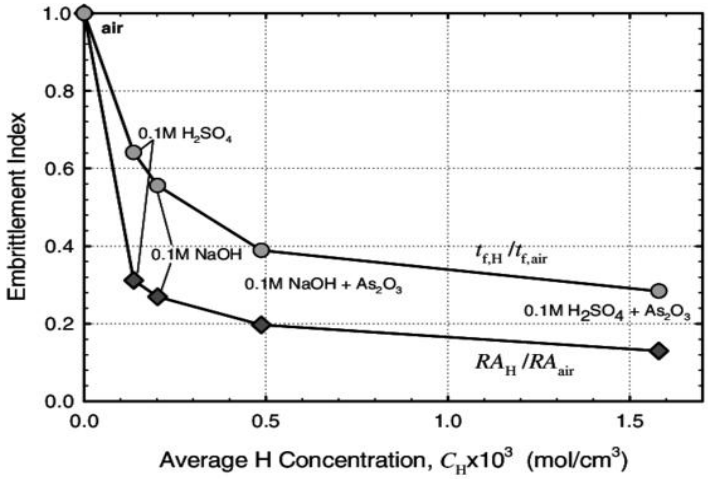

Figure 2: Effect of the average total concentration of hydrogen in the 23Cr–5Ni–3Mo duplex stainless steel on the embrittlement indexes (Zakroczymski et al., 2005).

The effect of hydrogen concentration on the $t_{f,H}/t_{f,air}$ and RA_H/RA_{air} ratios is shown in Fig. 2. both embrittlement indices demonstrated pronounced sensitivity to hydrogen concentration. The main decrease in ductility occurred already at a relatively low hydrogen concentration—about $0.2 \cdot 10^3$ mol/cm^3 i.e. about 26 ppm wt. A further increase of hydrogen concentration caused lower decrease in ductility. Therefore, one may suppose that the presence of hydrogen only as an interstitial solid solution may be sufficient to generate the considerable degradation of duplex stainless steel during its straining (Zakroczymski et al., 2005).

1.6.1 Hydrogen-Enhanced Local Plasticity (HELP)

Beachem first proposed the concept of hydrogen-enhanced plasticity in 1972, and it was consequently advanced through the work of Birnbaum and collaborators. The premise of the mechanism is that hydrogen assists the deformation processes, but only locally where hydrogen is present in sufficient concentrations, leading to fracture which is macroscopically brittle in appearance and behaviour (Martin, Dadfarnia, Nagao, Wang, & Sofronis, 2019).

Hydrogen is strongly bound to dislocation cores, this results in the formation of an atmosphere of hydrogen, which can resemble Cottrell carbon atmospheres. Dislocation motion is found to be accelerated in the presence of hydrogen. The mobility of the dislocations is usually increased, with 2–10-fold increases having been recorded, depending upon the material. This increase in mobility is due to the hydrogen atmosphere altering the stress field

of dislocations, allowing dislocation motion at lower stresses. It is rationalized that HELP led to an increase in the dislocation density and activity close to the boundaries, which resulted in modification of the boundary structures (Martin et al., 2019).

According to linear elasticity and finite element calculations, H can provide a shielding effect which reduces the repulsive force acting between edge dislocations and other obstacles (e.g., other parallel edge dislocations with Burgers vectors of the same sign, precipitates and interfaces). Such reduction is associated with the volumetric strain induced by H entering the lattice and the H-induced change of the constitutive moduli. In this regard, the concentrated H near the tips of either brittle or ductile cracks will produce a highly localized plastic zone, which makes the materials readily achieve the plasticity limit and promotes the formation of damages as shown in figure 3 (Sun et al., 2021).

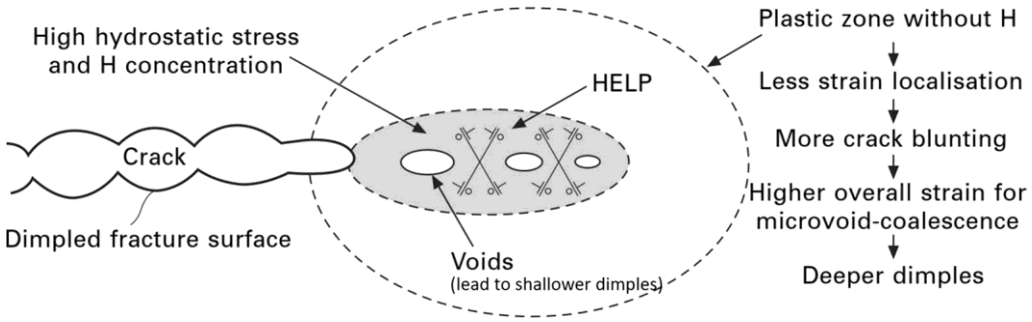

Figure 3: Schematic diagram showing the failure mechanism induced by the HELP model (Sun et al., 2021).

1.6.2 Hydrogen-Enhanced Decohesion (HEDE)

Hydrogen-enhanced decohesion (HEDE) is one of the many mechanisms of hydrogen embrittlement, a phenomenon that severely impacts structural materials such as iron and iron alloys. The HEDE mechanism has been attributed to weakening of interatomic bonds, due to the charge transfer between H and the host metal atom (Azócar Guzmán & Janisch, 2024).

In the H-enhanced decohesion model, it is proposed that the presence of H decreases the cohesive strength of lattice planes or interface boundaries. The underlying mechanism, suggested by Troiano, is that the electron of the H atom tends to enter the unfilled 3d shell of the iron atoms, which then increases the interatomic repulsive forces, thus decreasing the

cohesive strength. The frequently reported embrittling sites due to the HEDE mechanism are grain boundaries or interphase boundaries (Sun et al., 2021).

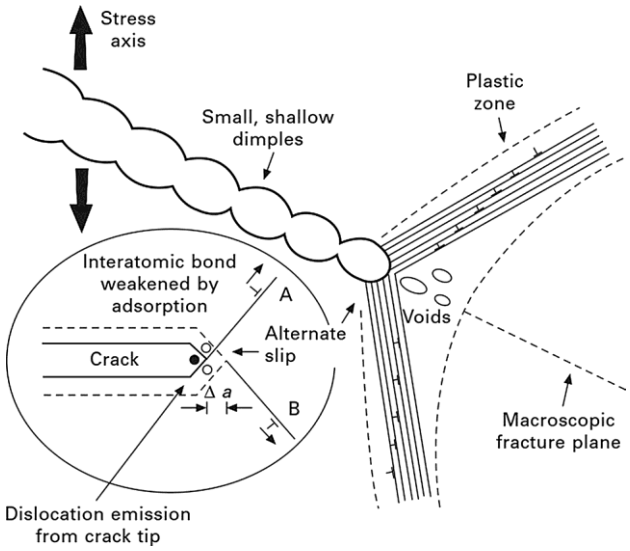

Figure 4: Schematic diagram showing the failure mechanism induced by the AIDE model (Δa, the length of the crack growth) (Sun et al., 2021).

1.7 Testing Methodologies for Hydrogen Embrittlement Evaluation

Hydrogen is prone to diffuse into materials, and even infinitesimals concentrations of hydrogen (<1 ppm) can gradually lead to a condition for embrittlement. However, it has become imperative to determine the presence of hydrogen within materials, ensuring accurate quantification, even at the level of measurement of single atoms. Molecular hydrogen undergoes reactions with small number of chemical elements but, once in a radical form, it exhibits interactions with numerous (Sobola & Dallaev, 2024).

1.7.1 Measurement of Hydrogen Content: Thermal Desorption Spectroscopy (TDS)

TDS tests are usually applied to quantify the binding energy of hydrogen interstitial trap sites in metallic alloys. In summary, the TDS test generally comprised of the following stages: Use of electrochemical and gaseous methods to charge the sample; Subjecting the sample to a constant rate and determining the flux molecules via desorption of hydrogen atoms with respect to temperature by employing a mass spectrometer (Raina et al., 2017).

Hydrogen TDS analysis is the study of hydrogen redistribution in the steel. The outcomes of the TDS was performed according to the procedures 1 and 2 measurements shows a number of hydrogen redistribution within the sample material during the AVC's dwelling

time of about 15 min as depicted in the figure 5 a, the first hydrogen desorption rate is quantified at RT is there for almost smaller a three times in the pre-cooled samples when compared to those ones that measured without cooling (Fangnon et al., 2020).

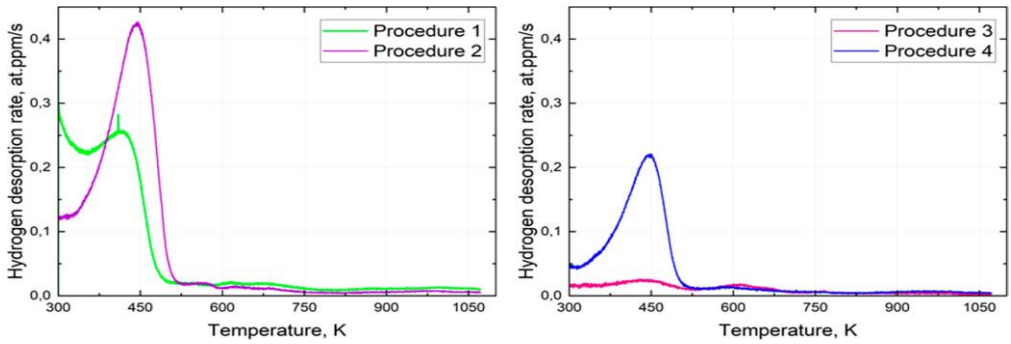

Figure 5: TDS curves corresponding to measurement procedures 1, 2, with the same AVC dwelling time = 15 min (a) and procedures 3, 4, with the same AVC dwelling time = 60 min (b) (Fangnon et al., 2020)..

1.7.2 Mechanical Testing: Slow Strain Rate Testing (SSRT) Approach

This method, developed by parkins, encompasses of applying to a sample a strain at a constant rate slow (usually 10^{-8} to 10^{-4} mm. s^{-1}) up to the point of failure occurs. The time to rupture is lined with the metal plasticity, that is relative elongation and decrease surface area. Regarded as a screening method, SSRT when compared with to the traditional method, it has the advantage of a method of the rupture occurs most often take place in a few tens of hours (Vargel, 2020).

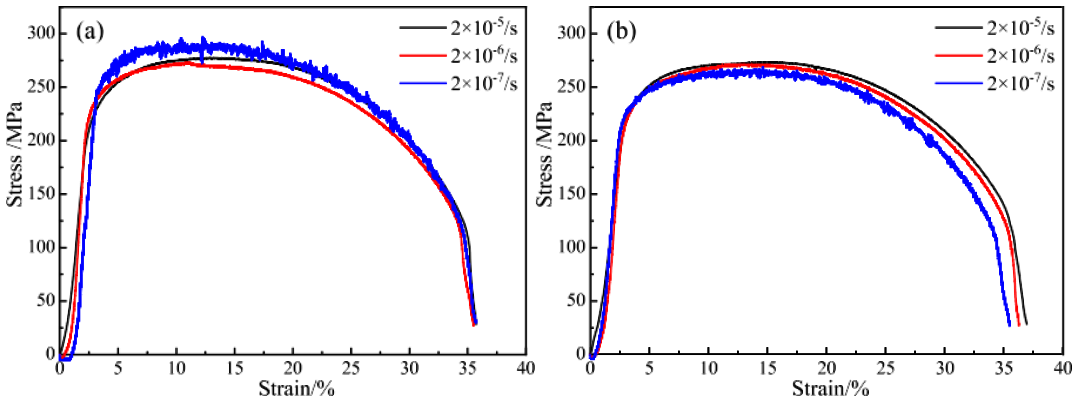

Figure 6: Stress–strain curves of TP439 SS during the SSRT (**a**) in air at 500 °C and **b** in water vapor at 500 °C s (F. Li et al., 2024)

Figure 6 shows a temperature of 500°C, the stress- strain rate curves of TP439 SS during the SSRT. The stress-strain curves of the sample fell slightly as the strain rate declined from

2×10^{5}/s to 2×10^{-6}/s. However, the curves showed a notable increase in the curves at the strain rate of 2×10^{-7}/s as shown in figure 6 a. At 500 °C temperature under water vapour environment, the curves of the specimen showed a similar trend to that of the observed in air when the strain rate decreased from 2×10^{-5}/s to 2×10^{-6}/s. However, the curves showed an opposite trend compared to that of the air when the strain rate dropped to 2×10^{-7}/s as shown in figure 6 b. at the same time, a serrated behaviour was observed in the sample curved at a strain rate of 2×10^{-7}/s (F. Li et al., 2024).

1.7.3 Electrochemical Hydrogen Charging Techniques

Electrochemical hydrogen charging provides an efficient approach to study he hydrogen embrittlement of steels, which offers a high concentration of hydrogen in a short duration with controllable charging parameters. Several studies have comprehensively explored the impacts of hydrogen charging on mechanical properties of steels. According to Arniella et al., that for 2205 DSSs, the hydrogen embrittlement increase in the index was associated with increasing hydrogen charging current density and hydrogen content. As elucidated by Wang et al., for high strength steels, an expanded diffuse hydrogen content correlated with a drop in notch tensile strength, where the extent of reduction became more evident with increasing stress concentration coefficients (Dan, Shi, Tang, & Wang, 2024).

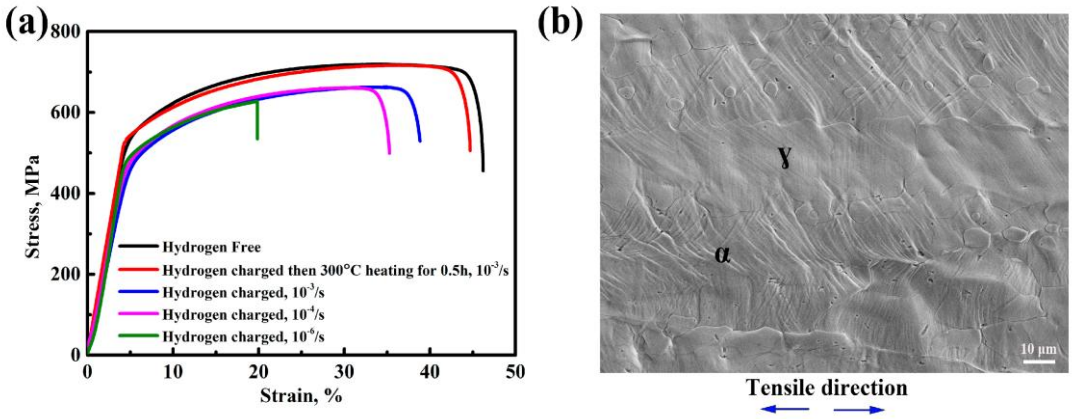

Figure 7: The nominal stress-strain curves of without hydrogen and with hydrogen under different strain rates (**a**); Sample surface for the hydrogen-free sample after fracture (Kan, Yang, & Li, 2019).

Figure 7 shows the nominal stress-strain curves and sample surface morphology after fracture of the hydrogen-free and hydrogen pre-charged specimens. As can be observed from

Figure 2a reveals that hydrogen pre-charging exhibited in a substantial decrease in elongation relative to that of the uncharged specimen. As shown by the blue and pink lines in the figure 7a, the plastic was substantially decreased after hydrogen charging at a high strain rate of 10^{-3} s^{-1} and 10^{-4} s^{-1}. As evidenced by the green line the plastic loss was more serious at a strain rate of 10^{-6} s^{-1}. A greater loss of elongation as the strain rate decreased. However, as represented by the red line, elongation was largely restored to the level as the hydrogen free sample when the hydrogen pre-charged specimen is subjected to tensile testing following a 0.5 h hold at 300 °C. The fractured surface of the sample was then inspected. Figure 7b illustrates the surface of the hydrogen-free sample, which remains free from microcracks (Kan, Yang, & Li, 2019).

Chapter 2: Materials and methods

2.1 Introduction

This chapter discusses the experimental setup conducted to investigate hydrogen embrittlement (HE) in using duplex stainless steels. This material has a corrosion resistant, characterized by distinct microstructural characteristics and the interaction of hydrogen varies depending on their crystallographic structures. The study aims to investigate or assess the susceptibility to Hydrogen embrittlement within hydrogen enriched environments by utilizing mechanical testing, hydrogen charging and microstructural analysis.

The methodology includes SSRT, and TDA to evaluate or study hydrogen-induced degradation and estimate hydrogen content. The empirical is intended to show the role of microstructural structures, such as grain size, and phase stability, influences hydrogen trapping and mechanisms of embrittlement. Therefore, this chapters outlines the study area, data collection, procedures, and analytical tools employed to obtain these objectives.

2.2 Materials and Chemical Compositions

In this research experiment, the chemical compositions of the DSS summarised in table 3. The material was obtained directly from DEW Swiss steel, a leading European steel manufacturer recognised for its high quality and reliable traceable materials.

Table III: Chemical compositions of the DSS

Unified Numbering System (UNS)	European Number (EN)	Cr (wt. %)	Ni (wt. %)	Mo (wt. %)	N (wt. %)	PREN (wt. %)
S82441	1.4662	24	3.6	1.6	0.27	33.60

The material is characterized by its special two-phase microstructure, comprising near-equal distributions of ferrite and austenite phases. This balanced structure results in combination of high mechanical strength and corrosion resistance provided by the ferrite phase, while the austenite phase offers high ductility and toughness.

The steels from DEW SWISS steel were selected particularly for its balanced chemical compositions, which is optimized to ensure a near-equal 50:50 distribution of austenite and ferrite phases. Alloying elements, including, nickel (Ni), molybdenum (Mb), and Nitrogen

(N), enhance both mechanical strength and corrosion resistance while also affecting hydrogen solubility and diffusion behaviour. This composition alloy is particularly appropriate for investigating the mechanisms of hydrogen embrittlement phenomena under the defined experimental conditions.

2.3 Metallographic preparations

In this research experiment, the metallographic preparation of the duplex stainless steel sample followed step by step systematic approach to ensure that dual-phase microstructure (ferrite and austenite) revealed for microscopic analysis. Each step was done to reduce preparation-induced artefacts and preserve the materials ferrite-austenite phase balance which is essential for assessing the hydrogen embrittlement behaviour.

The first step of grinding was performed using silicon carbide (SiC) abrasive papers with progressively finer grit size (up to P2000) to minimize surface deformation. Coarser grit papers were used first to eliminate sectioning defects and ensured planarity, with subsequent finer grit incrementally improved the surface finish. To maintain the correct austinite-ferrite balance, grinding pressure and speed kept low to preserve the duplex phase proportions. After surface grinding, the samples are briefly rinsed under running water and cleaned in an ultrasonic bath in a beaker filled with ethanol for 1-2 min. and dried under the sample dryer.

(a) Grinding Machine (b) Ultrasonic bath (C) Dryer

Figure 8: The sample undergoes grinding process.

The final polishing was performed using colloidal silica on a suspension soft cloth to remove residual surface damage and reveal the true microstructure for analysis. This step removed the thin deformation layer left by earlier polishing stages, producing a high-quality surface ready for microstructural etching.

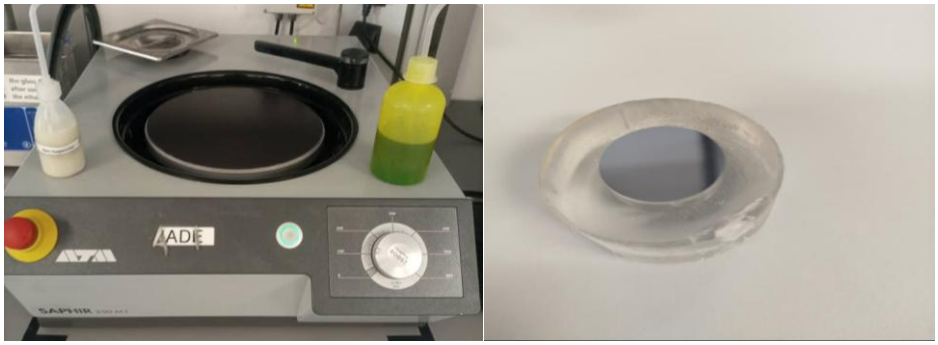

(a) Polishing machine (b) Sample

Figure 9: Sample undergoes polishing process

To make the duplex structure visible, etching was applied to reveal the microstructural contrast between the ferrite and austenite. The etchant (1000 ml warm distilled water, 200 g ammonium bifluoride, 5 g potassium disulfide) reacted selectively with ferrite and austenite phases, improving microstructural contrast, facilitating phase fraction analysis and grain boundaries via optical microscopy.

2.4 Strain Stress Rate Testing (SSRT)

Slow-Strain-Rate-Testing (SSRT) is an experimental method used to investigate how the hydrogen embrittlement susceptibility of metallic materials under regulated strain conditions, such as duplex stainless steel. In this study, SSRT was applied to the sample that had been hydrogen pre-charged or were charged in-situ. The principle involves deforming a specimen at a slow and constant extension rate until fracture occurs, allowing observation of how hydrogen affects ductility, tensile strength, and fracture behaviour compared to uncharged specimens.

Figure 10: SSRT machine

The testing was conducted on samples with standardized geometries (as prepared during metallographic preparation), mounted in a tensile testing machine capable of applying a precisely controlled strain rate. According to the methodology referenced in the thesis, typical strain rates used in SSRT at a speed of 5×10^{-6} s^{-1}. In this work, the selected rates aimed to be slow enough to allow hydrogen diffusion and trapping mechanisms to act during deformation, which makes embrittlement effects more visible. The process involved clamping the sample securely, starting the test by applying tensile load, and continuously recording stress–strain data until rupture.

2.5 Electrochemical Hydrogen Charging

Electrochemical hydrogen charging is a systematic and efficient method used to diffuse hydrogen uptake in metallic materials to investigate the phenomena of hydrogen embrittlement. In this study, the method was applied to the sample to replicate hydrogen-rich service conditions.

The charging process was conducted in a galvanostatic mode, using an acidic medium of sulfuric acid (0.05 M H_2SO_4), which facilitates the dissociation of hydrogen ions at the specimen surface under a constant current supplied by a DC power source with constant current.

The setup comprises a platinum counter electrode, the test specimen serving as the cathode, immersed in an electrolytic bath containing a sulfuric acid solution (H_2SO_4) with 1.4 g/l thiourea. Figure 11 illustrates this configuration, which leads to higher hydrogen concentration on specimen surface, where hydrogen atoms can diffuse into the material, thereby aiding in the analysis of hydrogen trapping and diffusion mechanisms.

Figure 11: Electrochemical hydrogen charging

2.6 Thermal Desorption Analysis (TDA)

Thermal desorption analysis (TDA) is a commonly used method to determine the quantity of hydrogen present in metals. Therefore, in this study, TDA was employed to investigate the H_2 concentration in duplex stainless steel after electrochemical charging. The process involves first charging the specimens with hydrogen, then heating them in a controlled manner to release the absorbed hydrogen, which is subsequently detected and measured. Figure 12 is showing Galileo G8 from company Bruker which is used in this study. The heating rate of 0.3 k/s was chosen and samples were heated up to temperature of 800 °C.

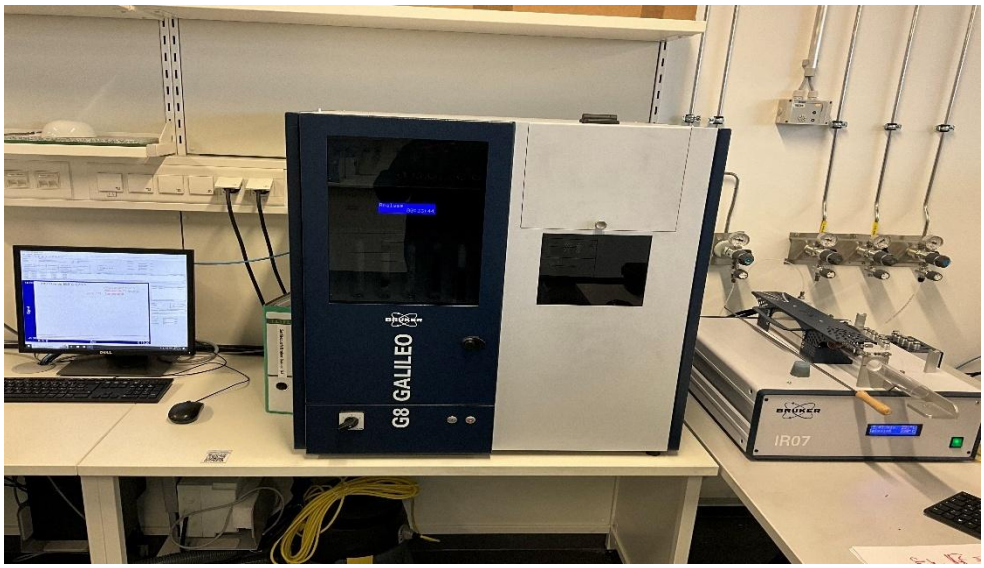

Figure 12 : TDA machine

To perform the analysis, each sample fully charged with hydrogen was directly inserted into the G8 GALILEO system to avoid hydrogen outgassing. The sample were set into a water-cooled electrode furnace, and the chamber was purged with an inert gas helium to remove the atmospheric influence. The G8 GALILEO utilizes thermal desorption mass spectrometry (TDMS), which provides the capability to detect hydrogen molecules as they desorb from the sample while being heated. The Smart Molecule Sequence of the system allows direct and accurate determination of emitted gases, with no dependence on chemical conversion or correction algorithms. Internal reference channels and a regulated ion source system provide additional assurance in detection of hydrogen at parts per billion (ppb) levels. With the use of thermal conductivity detector (TCD) during the heating process, hydrogen evolution was kept under continuous observation, thereby enabling sensitive analysis of hydrogen trapping and the release behaviour. This approach provided a logical methodology to quantify the hydrogen content of duplex stainless steels and evaluate the hydrogen uptake of these alloys using a controlled experimental approach.

Chapter 3: Results and discussion

3.1 Introduction

This chapter includes the experimental results of microstructural characterisation, mechanical tests, and hydrogen contents analysis and fractography, which then followed by detailed discussions of their impacts. The main goals of this study were to assess the susceptibility of the EN 1.4662 DSS to hydrogen embrittlement, the correlation between microstructural features with that of the embrittlement mechanisms and examining the impact of heat treatments on hydrogen trapping and diffusion.

The outcomes are divided into four major parts, which are microstructural characterizations, mechanical properties, hydrogen content measurements and fractography. The results are discussed in the framework of established HE mechanisms, such as HELP and HEDE, as well as the key role of phase boundaries and alloying elements. This chapter aims to provide a deep understanding of HE within EN 1.4662 and thus providing integrated experimental evidence within theoretical frameworks to create a more thorough grasp from standard laboratory observations to practical industrial applications.

3.2 Microstructural Characterization

3.2.1 Before Annealing (As received)

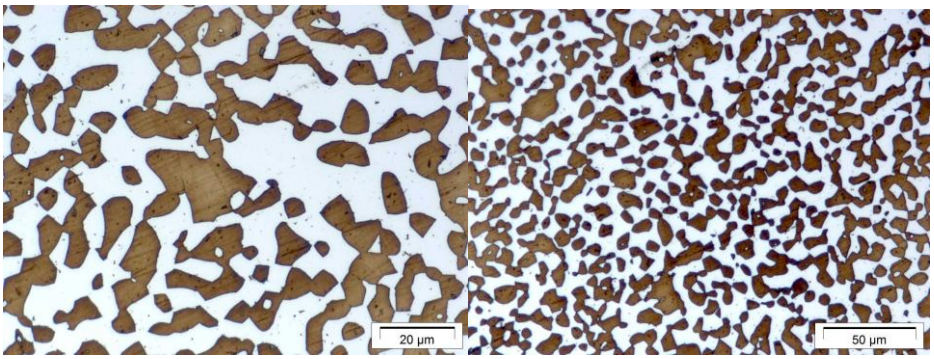

(a) (b)

Figure 13: As-received DSS microstructure showing irregular phase distribution, 500X

The microstructure of as-received state prior to annealing was analysed at varying magnifications through optical microscope to illustrate the phase distribution of duplex stainless steel. The outcomes make it evident that in the material phase, appearing the light area (ferrite), and phase material, appearing the dark area (austenite), are distributed throughout the materials. At the low magnification (20 µm), The characteristics of the austenite islands in a ferritic matrix are clearer. The austenite portions look rather elongated and pronounced

thereby emphasizing the distinct phase boundaries between the two phases. As no precipitates of secondary phase or otherwise any anomalies as observed in the figure 13 a, the material before annealing has a stable microstructure.

At high magnification (50 µm), the duplex structure seems to reach a uniform duplex structure of ferrite as a continuous film with isolated islands of austenite as shown in 13 b.

3.2.2 Annealing at 1050 ºC

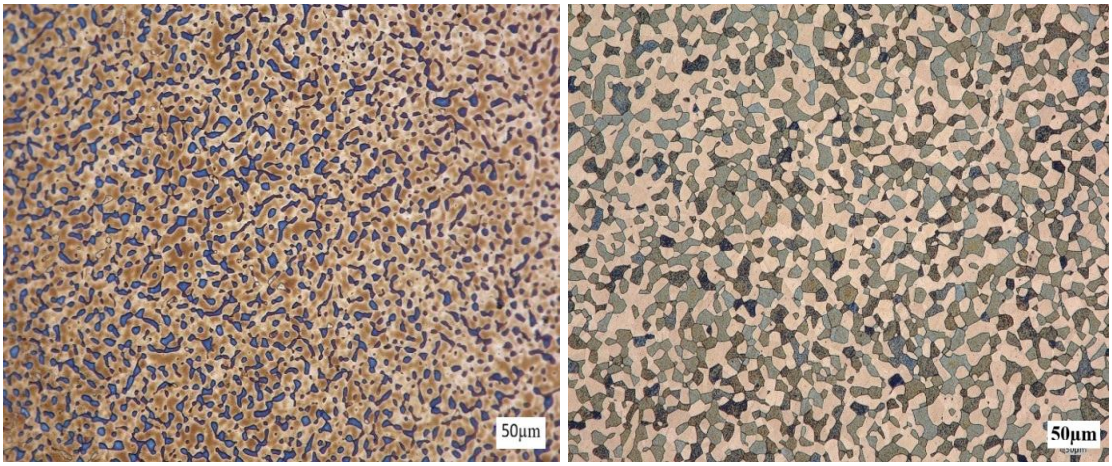

(a) (b)

Figure 14: The microstructure phase evolution after annealing (a) After annealing at 1050 ºC for 120 minutes, 500X (b) At 1050 ºC for 800 minutes, 500X

In Figure 14 a (scale 50 µm, 500 magnifications of microstructure after exposing to 1050 °C for 120 min) ferrite is seen in darker while austenite in lighter in contrast, and the duplex phase state distribution is relatively finely distributed. Whilst the phase balance remained reasonably close to the expected 50:50 for duplex stainless steels, however coarse irregular grains were obtained within the microstructure. The distinction of these phases is revealed as shown in the structure, for which the methodology of careful metallographic preparation consisting of low-speed sectioning with subsequent progressive grinding up to P2000 grit and final polishing with colloidal silica followed by selective etching enabled differentiation between each constituent phase. The finer grain size and higher density of interphase boundaries lead to more potential hydrogen-trapping sites, which could affect the hydrogen retention and embrittlement behaviour under a hydrogen rich-environment.

In figure 14 b (annealed at 1050 °C for 800 minutes, scale bar: 50 µm) shows a more homogenous equiaxed microstructure with increasing the grain size compared to Figure b.

This austenite fraction is rather close to 55% suggesting slight phase transformation in favour of austenite stability during the prolonged high-temperature exposure. Enhanced thermal treatment reduces both the defect density and internal stresses surrounding grain boundaries allowing them to be easily distinguished from one another. The decrease in microstructural disorder could influence hydrogen transport, which may result in either decrease density of trapping sites but also increased pathways for hydrogen mobility.

The microstructure of both magnifications at different time shows how the annealing duration at a constant temperature affects duplex stainless-steel microstructure. A thinner, more discontinuous network with a higher boundary density that also gives even more second phase-trapping possibility seen in figure 14 a. On the other hand, the coarser and phase-stable structure in fig b might have reduced hydrogen trapping but more diffusion potential. These microstructural differences, captured with high resolution across consistent magnification using optical microscopy, provide a foundation for linking grain size and phase distribution to hydrogen embrittlement susceptibility.

3.3 Mechanical Properties

3.3.1 Without Charging

Deformation profile of duplex stainless steel under slow constant loading, as depicted in SSRT results presented in Graph a (engineering stress-displacement) and Graph b (true stress-strain), for the “Without Charging” condition. A steep rise in engineering stress which denotes that the material will undergoes the elastic deformation up to yield point depicts in figure 15. The resulting gradual incline into the plastic region illustrates the ligaments can be deformed to higher strains while ensuring that high stress is sustained, (reaching a peak tensile strength of nearly 695 MPa). Considering the experimental data, uniform elongation continues to increase without necking, indicating a high ductility under non-hydrogen charging condition. The displacement axis depicts the sample undergoes a notable extension before failure, indicating strong resistance to mechanical fracture without influence of hydrogen.

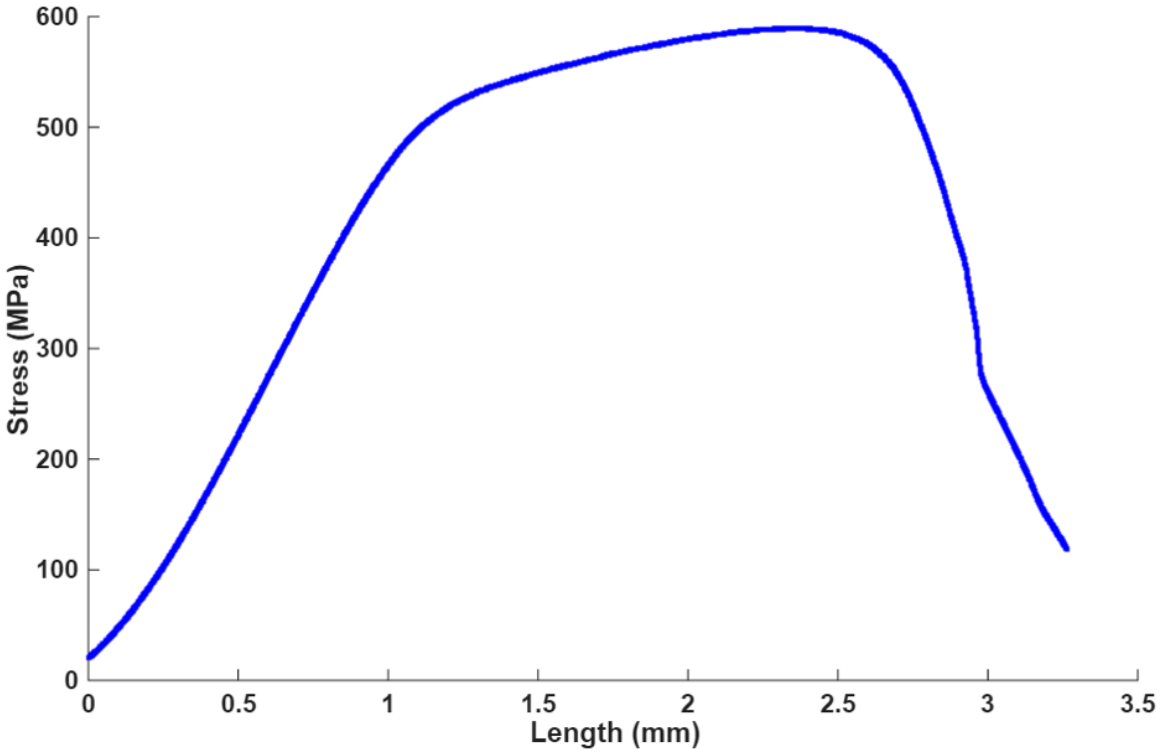

Figure 15: Engineering stress-displacement response of uncharged Duplex Stainless Steel

Graph 16, where engineering stress is plotted against engineering strain, provides even more clarity to this by taking into consideration the reduction in cross-sectional area during deformation. This high initial stress results from the rapid stress increase followed by a broad plateau spanning a large strain range typically indicating excellent sustained strain hardening capacity. The ultimate or maximum tensile strength measured was 695 MPa which corresponds to 25% uniform elongation proving the good combination of strength and ductility. The final decrease in stress would then be associated with fracture (and would naturally occur only after further extensive plastic straining) as can be seen by the ductile nature of the rupture surface revealed during later examination (SEM data). This is an indication of the intrinsic embrittlement resistance in the alloy in the absence of hydrogen, under strain rate (5×10^{-6} s^{-1}) and initial state SSRT conditions.

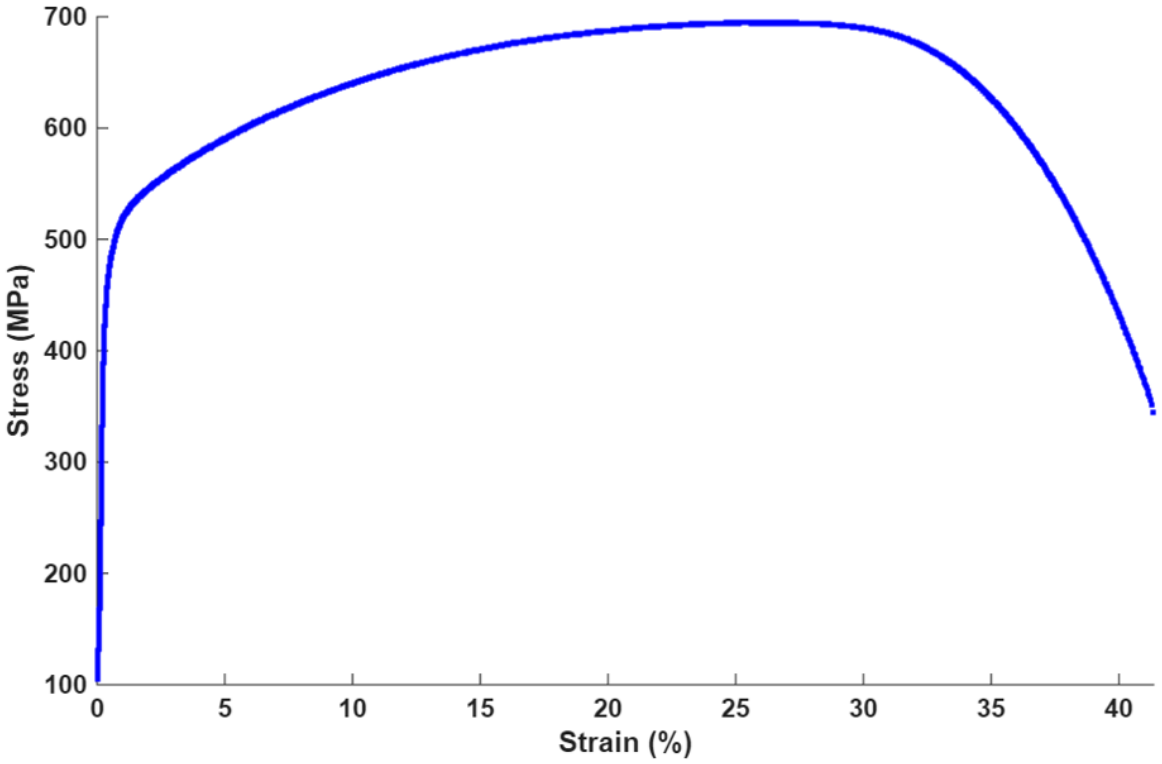

Figure 16: Stress-strain behaviour of uncharged Duplex Stainless Steel

3.3.2 With Hydrogen Charging

The measured engineering stress–displacement curves are shown in Figure 17, where the hydrogen-charged specimen exhibits lower peak stress (approximately 590 MPa) before fracture. Hydrogen charging is expected to start localisation and failure of strain earlier as shown by a reduced plastic deformation range after the elastic region. This behaviour is consistent with a progressively lower fraction of deformation that the material can accommodate once yielding starts — a manifestation of expected embrittlement as hydrogen moves into solution.

The stress–strain curve (Figure 18) reinforces these observations, incorporating a reduction in cross-sectional area during deformation. The hydrogen-charged material shows a much lower maximum stress and a considerably reduced uniform elongation. A severe reduction in ductility and strain-hardening response is clear from the pronounced decrease. Thus, the steepness of decreasing stress after its peak in hydrogen-charged condition is strong evidence for a limited amount of post-necking deformation, demonstrating a behaviour to undergo brittle failure rather than large strain. This behaviour is in line with the generally enhanced crack initiation and propagation rates determined with the SSRT methods found for hydrogen-embrittled alloys during testing at low strain rates.

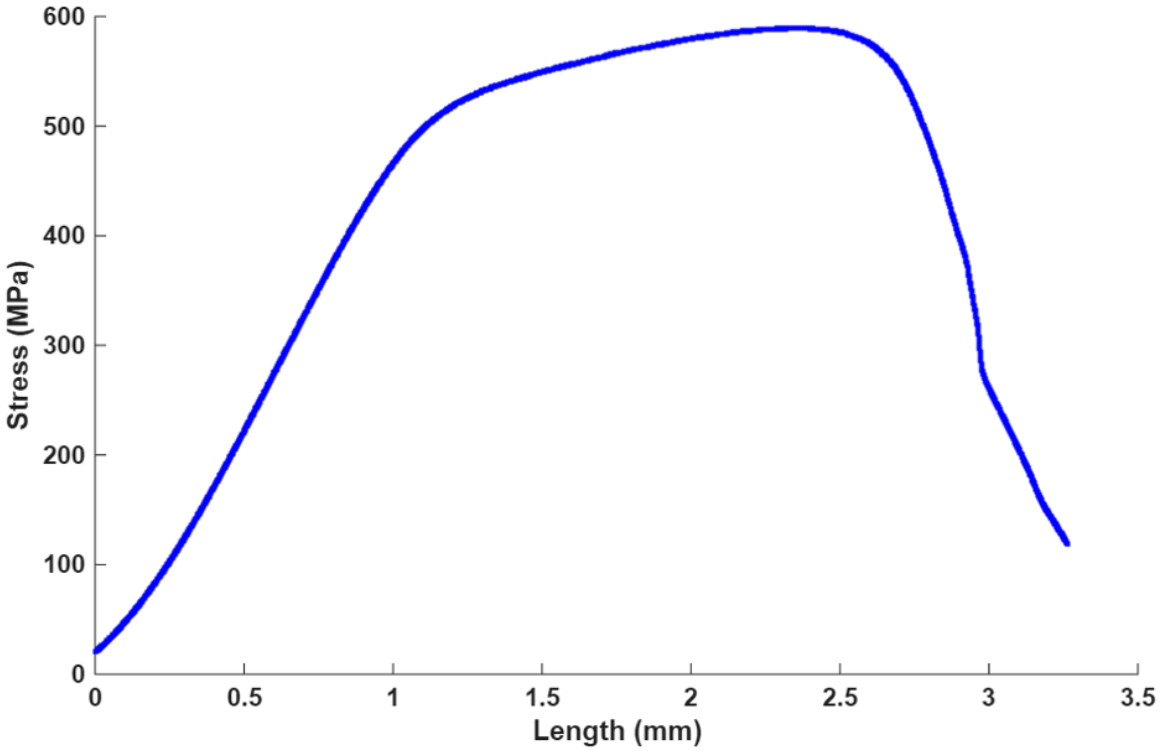

Figure 17: Engineering stress–displacement curve of Duplex Stainless Steel under hydrogen-charged condition

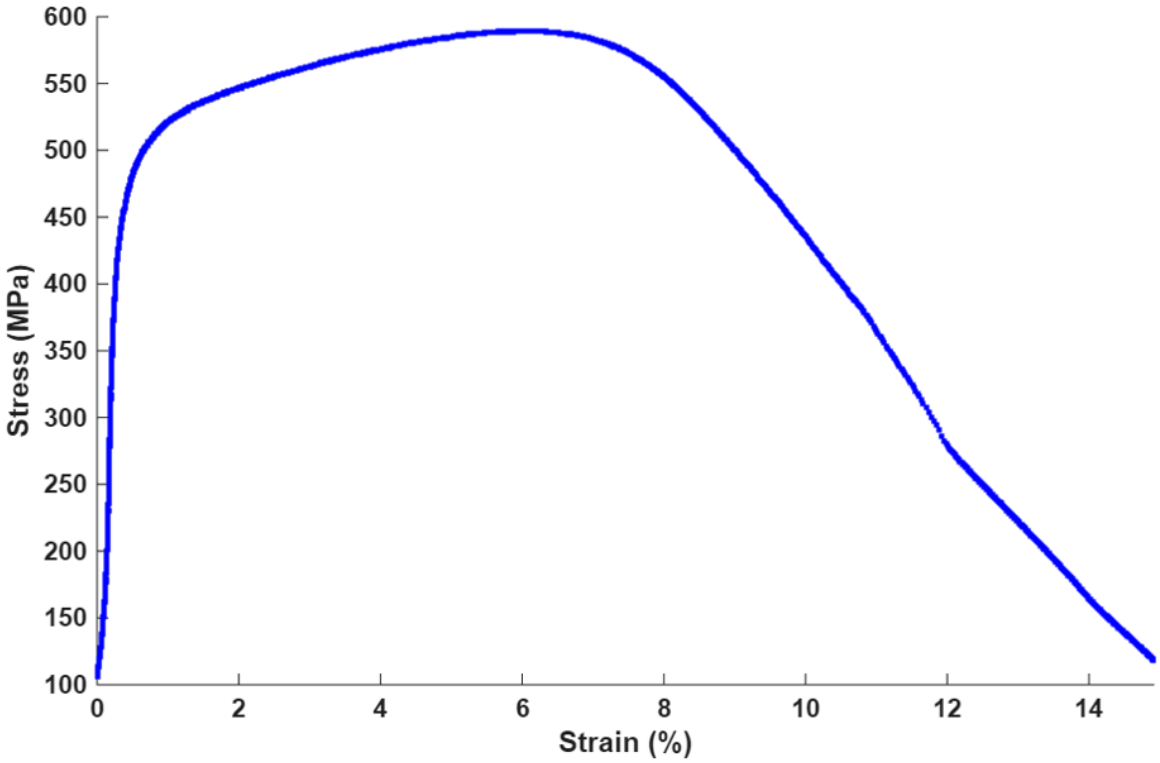

Figure 18: Stress–strain curve of Duplex Stainless Steel under hydrogen-charged condition

3.3.3 With Charging and Without Hydrogen Charging

The differences of the charged and uncharged specimens are shown in the Fig 19. The uncharged material extends almost 9 mm before fracturing indicating extensive plastic deformation. In contrast, the hydrogen-charged sample breaks at only 3 mm elongation, demonstrating that hydrogen embrittlement is significant. These findings are consistent with the hydrogen-embrittlement phenomenon and indicate that the presence of hydrogen limits the plastic deformation of the material; it breaks earlier and more abrupt fracture.

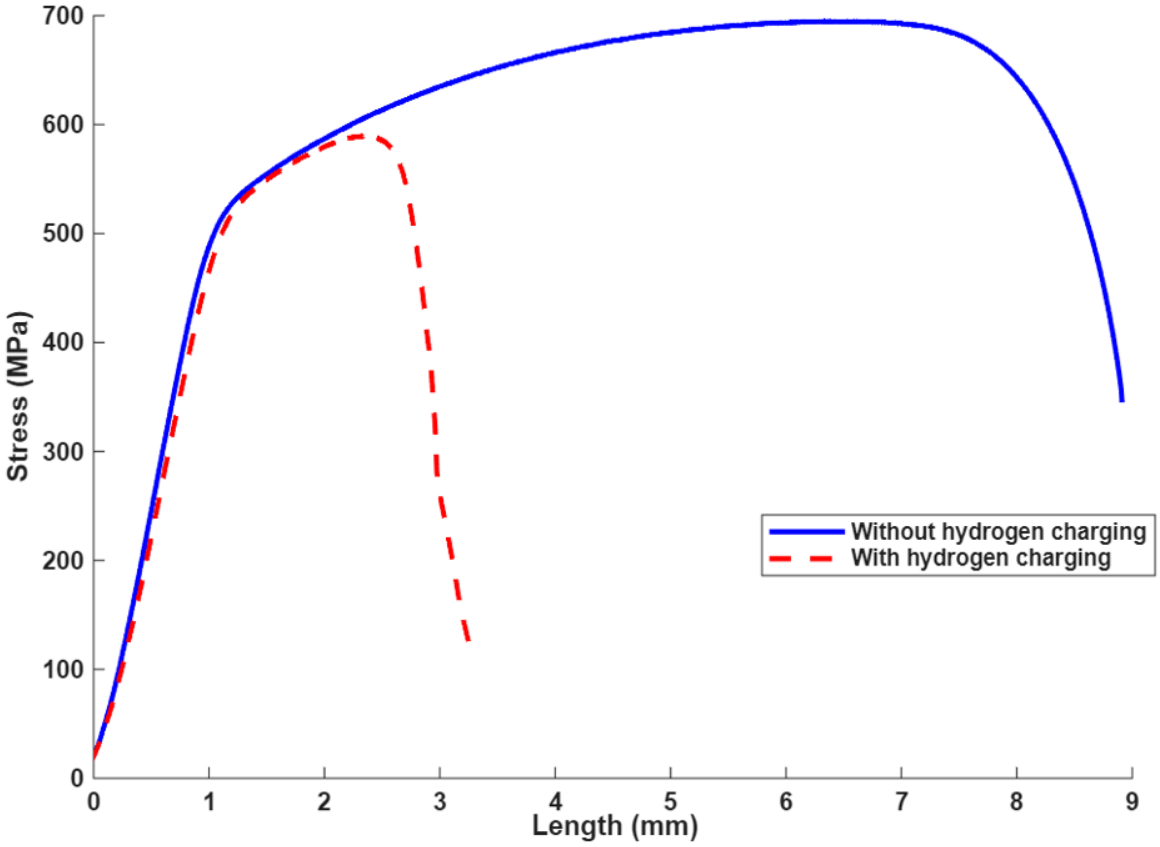

Figure 19: Engineering Stress-Displacement Response of Uncharged and Charged Duplex Stainless Steel

The (SSRT) curves of specimens with and without hydrogen charging show the distinct mechanical behaviours. At uncharged state, the first tensile stress–strain curve grew steadily with increasing strains and reached the maximum tensile stress value about 695 MPa, after that decreased relatively slowly, it indicates high resistance to the occurrence of plastic

deformation of the material before failure. In contrast, the hydrogen-reduced sample continues to have fallen stress after it peaks at around 590 MPa and has a much lower strain to failure. This behaviour indicates that the deformation process and the ductility are strongly altered by the hydrogen charging.

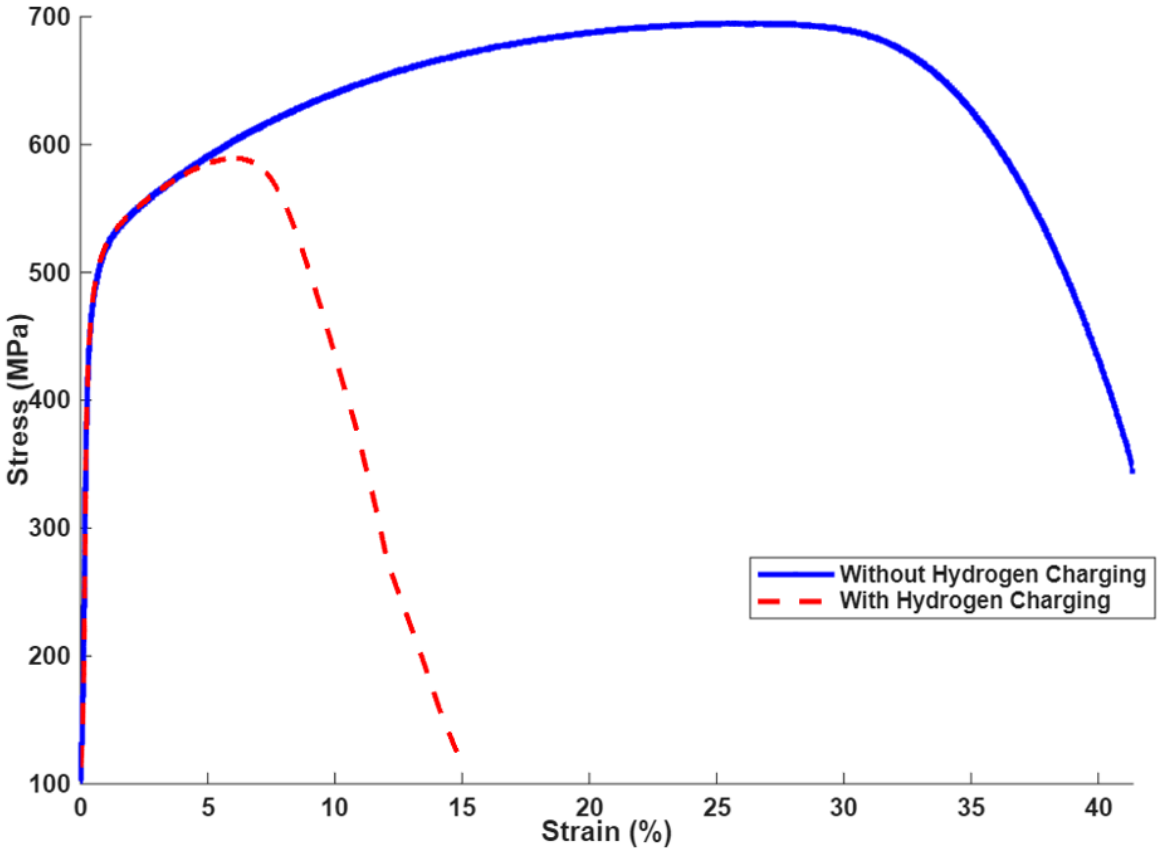

Figure 20: Stress–strain curve of Duplex Stainless Steel under hydrogen-charged and uncharged condition

Table IV: SSRT with and without hydrogen charging

Parameters	Without charging	With charging
Yield strength (MPa)	474	484
Tensile strength (MPa)	695	590
Uniform elongation (%)	25.0	5.9
Total elongation (till failure) (%)	41.2	14.8
Total time (s)	67056,9	24518,0

These observations are further confirmed by the mechanical parameters table. Although the yield strength under hydrogen-uncharged and hydrogen-charged conditions differs minimally (474 MPa in uncharged condition and 484 MPa in charged condition), the tensile strength decrease evidently under hydrogen charging. The total and uniform elongation respectively decrease from 41.2% and 25% in the uncharged state to 14.8% and 5.9% charged. Moreover, the time to total failure reduces quite dramatically from 67,056 seconds to 24,518 seconds in the presence of hydrogen. Taken together, these results suggest that hydrogen diminishes the ductility and fracture resistance more than the yield strength, even though the yield strength is almost unchanged, corresponding to the hydrogen embrittlement features.

3.4 Hydrogen Content Analysis

TDA was used to analyse the hydrogen content that had charged the duplex stainless-steel sample, and quantification of total hydrogen levels in duplex stainless-steel specimens released up to a certain temperature. Fig 20 depicts the rate at which hydrogen is released with time shows that the desorption peak around 400–900 s reaches its maximum in the region of about 0.034 ppm/s. This sharply rising and dropping part of the curve represents saturation points, i.e. most of the absorbed hydrogen is desorbed by approximately the same time so that one or two major trapping sites are dominant in this analysis section, with very similar binding energies. As shown in below graph, the total hydrogen observed on test piece writing is 12 ppm.

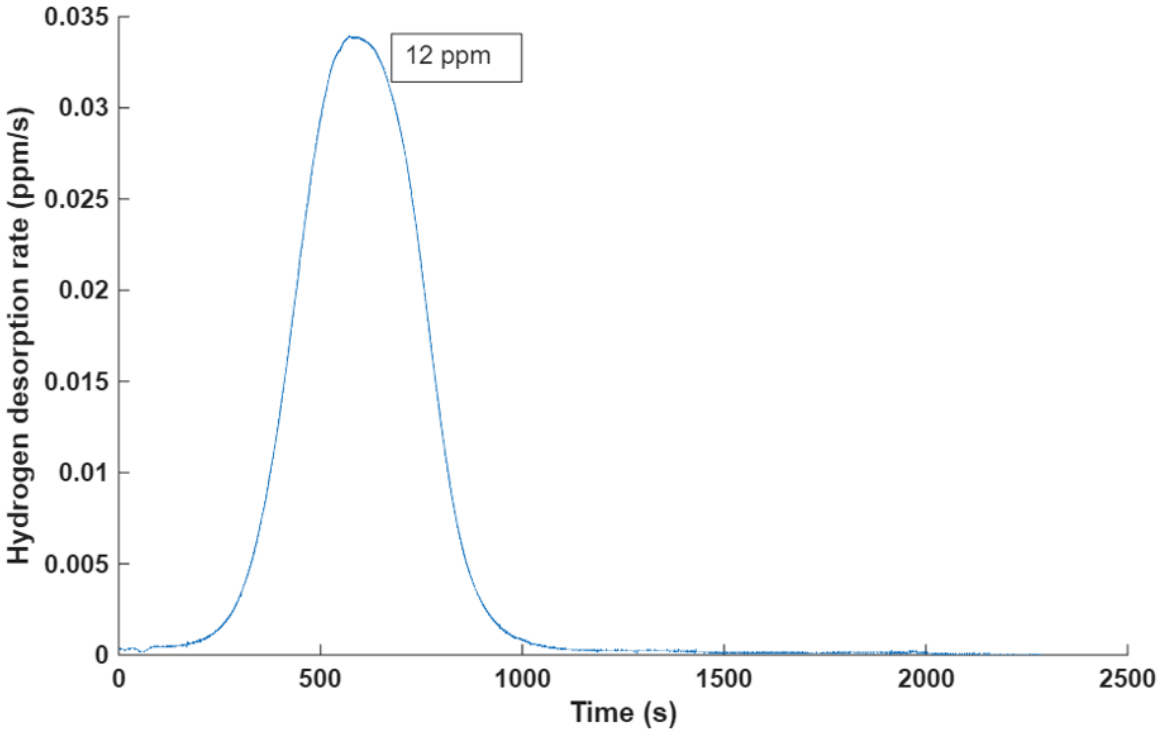

Figure 21: Hydrogen desorption rate as a function of time for Duplex Stainless Steel

The graph 21 b plotted with respect to temperature which shows an average thermal activation energy necessary to release hydrogen. The major peak appears around 280 °C and can be attributed to the release of hydrogen from moderately strong traps that is commonly attributed to dislocations, grain boundaries or phase interfaces in a duplex stainless steel. The absence of multiple peaks indicated that hydrogen was mainly trapped in traps with similar energy levels as opposed to a broad distribution of traps characterized by distinct stabilities, under the experimental charging conditions. After that the desorption rate went on to almost zero, such a drastic drop means that there were no deeper or/and stronger traps or exist in very low concentration.

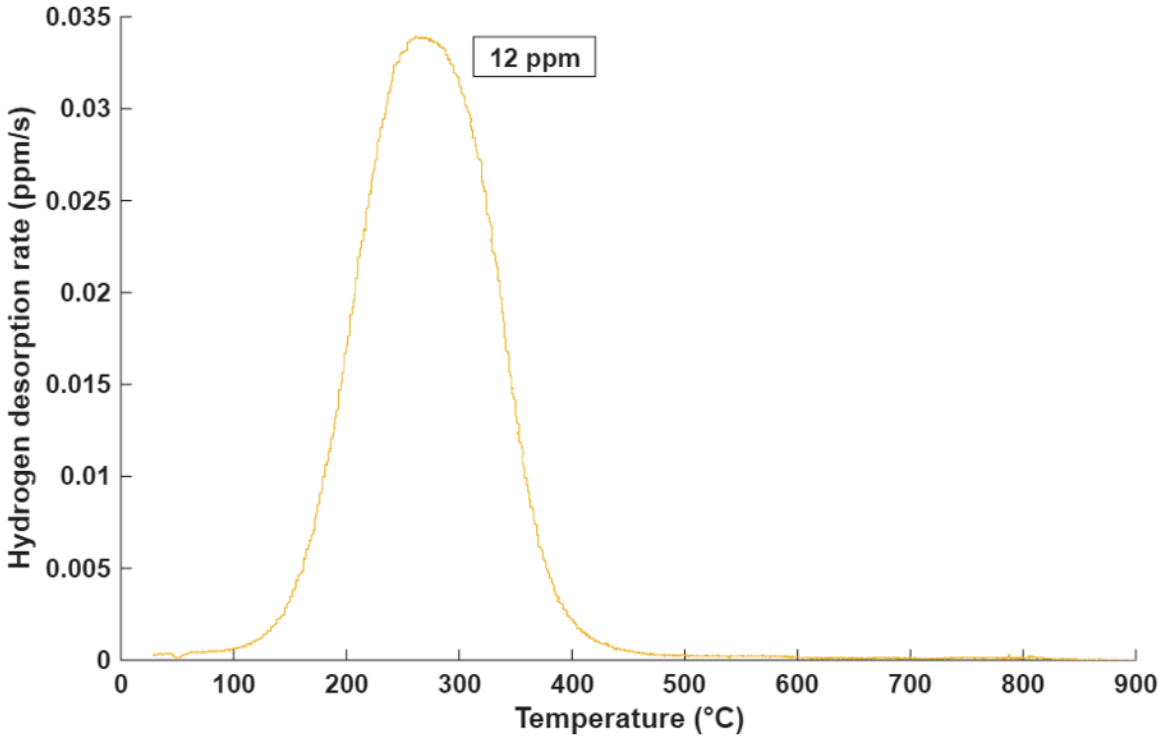

Figure 22: Hydrogen Desorption Rate as a Function of Temperature for Duplex Stainless Steel

Results indicate that hydrogen content in the steel was homogenous and measurable after the electrochemical charging methods, with desorption profiles consistent with trapping sites within the microstructure. This correlation between times and temperature shaped curves indicates first-order desorption kinetics through a single major trapping level for hydrogen release from these samples. This characterisation of hydrogen retention and release behaviour created a foundation upon which the TDA results to mechanical performance changes demonstrated in SSRT tests could be related, as hydrogen stored in these sites can be mobilised under service temperatures or during mechanical loading leading to embrittlement susceptibility.

3.5 Fractography

3.5.1 Uncharged SEM Image

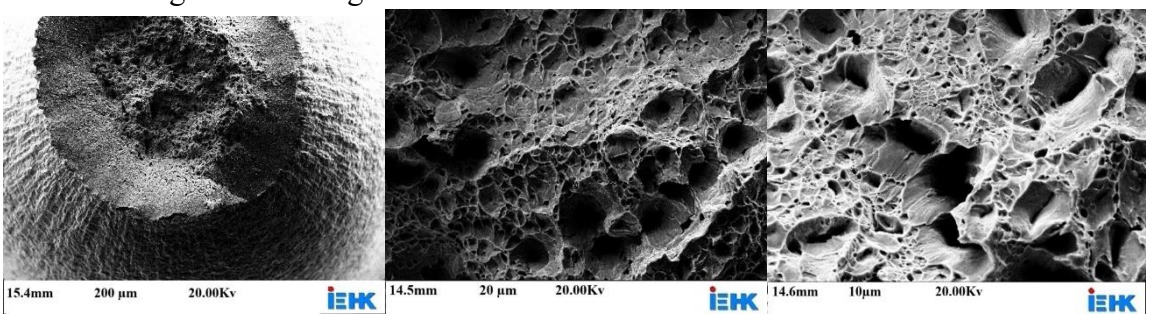

(a) (b) (c)

Figure 23: Scanning electron microscope images of without hydrogen charge sample (a) SEM image 29X (b) SEM image 100X (c) SEM image 500X

Utilising scanning electron microscopy (SEM), the uncharged specimen fractography exhibits typical features relate to ductile fracture at various magnifications. At lower magnifications of 50x, 15.4 working distance of 15.4mm, 200 µm of bar scale and voltage of 20kv as shown in fig(a), the general fracture surface presents a cup-and-cone feature characteristic of a material with a substantial plastic deformation prior to failure. This general observation emphasizes that the duplex stainless steel could accommodate significant strain without early crack nucleation, which suggests the ductility of the duplex stainless steel was good in uncharged environment.

In the high magnification of 500x, 14.5mm working distance, 20µm of bar scale and voltage of 20kv as shown in fig(b), the broken surfaces are covered by relatively dense dimples of various sizes, the typical evidence for the formation of micro-voids and their coalescence by deformation. The even distribution of these dimples implies that the fracture was ductile as opposed to instantaneous brittle fracturing. This pitted pattern indicates that several microstructural features served as the origin of voids, but allowed stable void growth before ultimate failure, which again is consistent with the ductile nature of the failure without hydrogen charging.

At the highest magnification of 1.00kx, 14.6mm working distance, 10 µm of bar scale and voltage of 20kv as shown in fig(c), finer features of the fracture surface are evident such as sub-dimples and regions with distinct tearing ridges. These characteristics establish that the

material was subjected to localized plastic deformation up to the rupture, behaviour common to metals of adequate toughness and resistance to embrittlement. It can be concluded that, under slow strain rate testing without hydrogen charging, the duplex stainless steel still features a ductile fracture mode from these SEM images. This result confirms the inherent toughness of the material and the fact that in the absence of hydrogen, embrittlement does not occur.

Table V**:** Fracture Surface Characteristics of Uncharged DSS at Varied Magnifications

Magnification	Working distance (mm)	Scale bar (µm)	Voltage (Kv)
50x	15.4	200	20.00
500x	14.5	20	20.00
1.00kx	14.6	10	20.00

3.5.2 Charged SEM Image

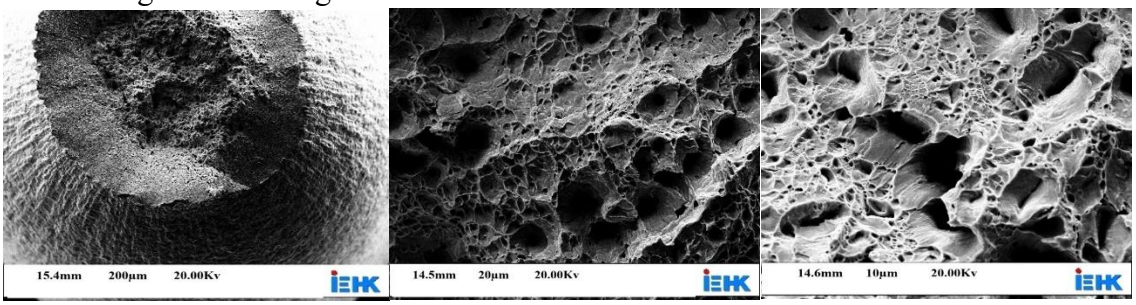

(a) (b) (c)

Figure 24: Scanning electron microscope images of hydrogen charged sample (a) SEM image 100X (b) SEM image 500X (c) SEM image 1.00KX

SEM fractographic examination for the hydrogen-charged sample after slow strain rate testing reveals an entirely different fracture surface appearance as compared to the uncharged status. A rougher more irregular fracture surface with less definition of the uniform cup and cone profile is observed at low magnification of 100x, working distance of 17.0mm, 100 µm of bar scale and voltage of 20 kv as shown in fig 22 a. On the contrary, the central fracture region displays patterns of localised damage and of more inhomogeneous texture, which indicate that the hydrogen charging affected the fracture process and promoted embrittlement phenomena.

At a moderate magnification of 500x, 14.5mm working distance, 20 µm of bar scale and voltage of 20 kv as shown in fig 22 b , the fracture surface has less well-developed dimples and a less regular void structure. Most voids appear to be expanded and linked, reflecting coalescences that are apparently less controlled than in the free state. The anomalous appearance of these small dimples is indicative of the role of hydrogen in the weakening of microstructural features and the premature growth and linking of voids and subsequent loss of ductility in during deformation.

At higher magnification 1.00 kx, 14.6 mm working distance, 10 µm of bar scale and voltage of 20 kv as shown in fig 22 c, smaller scale structures of the surface show network of shallow dimples and tearing features, incorporating microcracking along the fracture surface.

Table VI**:** Fracture Surface Characteristics of charged DSS at Varied Magnifications

Magnification	Working distance (mm)	Scale bar (µm)	Voltage (Kv)
50x	15.4	200	20.00
500x	14.5	20	20.00
1.00kx	14.6	10	20.00

CONCLUSIONS AND PERSPECTIVES

4.1 Conclusions

The impact of hydrogen on the mechanical behaviour and fracture mechanisms of DSS was well investigated through electrochemical charging, slow strain rate tensile (SSRT) testing, thermal desorption analysis (TDA), and fractography. It was found that hydrogen charging greatly affected the ductility reduction and the morphology of the fracture surface and had little effect on the yield strength. Analysis of the hydrogen desorption behaviour confirmed the existence of trapping sites possessing a moderate binding energy that are responsible for the slow release of hydrogen during mechanical loading.

Fractographic examination revealed the conversion from a fully ductile fracture mode (deep dimples and uniform mixing region) for the un–charged samples to a mixture of ductile and brittle fracture (irregular dimples and microcracking) for the charged ones. The occurrence of this change, combined with the low elongation and early fracture in the SSRT tests, clearly demonstrates the hydrogen embrittlement susceptibility of duplex stainless steels in the investigated conditions. These results confirm the initial hypothesis that hydrogen does have a large effect on fracture behaviour and embrittlement mechanisms, especially in ductility reduction and fracture mode changes.

In general, the study provide insight into the hydrogen embrittlement mechanisms in DSS. The inferences made provide further credence that hydrogen causes a loss of microstructural integrity and precipitates premature fracture. These results are valuable to both academic research and to industries employing duplex stainless steels in metal with hydrogenous environment.

4.2 Perspectives

Further study in the future will seek a more robust understanding through a wide range of experimental variables, such as varying changing times, current densities, and strain rates to better understand the correlation between hydrogen uptake and fracture. The use of various grades of duplex stainless steels, chemical compositions could also extend the scope and disentangle microstructural factors leading to the promotion, or either resistance, of hydrogen embrittlement. This could support to establish a broader guideline for material selection in hydrogen application.

A further suggested approach is to correlate experimental work to advanced characterization techniques including atom probe tomography (APT) to investigate hydrogen trapping at a nanoscale. Such techniques would enable a more detailed understanding of the microstructural features that trap and release hydrogen. Furthermore, using modelling techniques, such as finite element simulations, or hydrogen diffusion modelling may allow the embrittlement behaviour under service like conditions to be predicted, which will enhance further the applicability of this study.

Finally, this investigation could be expanded to include application-orientated testing (e.g., testing duplex stainless-steel components in simulated service condition: under high pressure hydrogen gas, at different temperatures and under cyclic loading). Such research would provide a link between laboratory scale results and industrial applications. In doing so, the results would not only validate the hypothesis under the more general conditions, but also provide practical guidance for the design, process and safe operation of materials in hydrogen-related infrastructures.

References

Adhe, K. N., Kain, V., Madangopal, K., & Gadiyar, H. S. (1996). Influence of Sigma-Phase Formation on the Localized Corrosion Behavior of a Duplex Stainless Steel. In *JMEPEG* (Vol. 5).

Azócar Guzmán, A., & Janisch, R. (2024). Effects of mechanical stress, chemical potential, and coverage on hydrogen solubility during hydrogen-enhanced decohesion of ferritic steel grain boundaries: A first-principles study. *Physical Review Materials*, *8*(7). https://doi.org/10.1103/PhysRevMaterials.8.073601

Boillot, P., & Peultier, J. (2014). Use of stainless steels in the industry: Recent and future developments. *Procedia Engineering*, *83*, 309–321. https://doi.org/10.1016/j.proeng.2014.09.015

Chemelle, P. (2011). The history of duplex developments,nowadays DSS properties and duplex market future trends. *World Iron & Steel*. https://api.semanticscholar.org/CorpusID:112754765

Choi, J. Y., Ji, J. H., Hwang, S. W., & Park, K. T. (2012). Effects of nitrogen content on TRIP of Fe-20Cr-5Mn-xN duplex stainless steel. *Materials Science and Engineering: A*, *534*, 673–680. https://doi.org/10.1016/j.msea.2011.12.025

Chou, S.-L., Tsai, M.-J., Tsai ', W.-T., & Lee, J.-T. (1997). Effect of nitrogen on the electrochemical behavior of 301LN stainless steel in H2S04 solutions. In *Materials Chemistry and Physics* (Vol. 51).

Duplex stainless steels. (n.d.).

Dwivedi, S. K., & Vishwakarma, M. (2018). Hydrogen embrittlement in different materials: A review. In *International Journal of Hydrogen Energy* (Vol. 43, Issue 46, pp. 21603–21616). Elsevier Ltd. https://doi.org/10.1016/j.ijhydene.2018.09.201

Fangnon, E., Malitckii, E., Yagodzinskyy, Y., & Vilaça, P. (2020). Improved accuracy of thermal desorption spectroscopy by specimen cooling during measurement of hydrogen concentration in a high-strength steel. *Materials*, *13*(5). https://doi.org/10.3390/ma13051252

Francis, R., & Byrne, G. (2021). Duplex stainless steels—alloys for the 21st century. *Metals*, *11*(5), 1–23. https://doi.org/10.3390/met11050836

Fujisawa, M., Mauchi, R., Morikawa, T., Tanaka, M., & Higashida, K. (2014). Influence of strain-induced martensite on tensile properties of metastable duplex stainless steels consisting of Fe-Cr-Mn-Ni and Fe-Cr-Mn-N. *Tetsu-To-Hagane/Journal of the Iron and Steel Institute of Japan*, *100*(9), 1140–1149. https://doi.org/10.2355/tetsutohagane.100.1140

Gouné, M., Danoix, F., Ågren, J., Bréchet, Y., Hutchinson, C. R., Militzer, M., Purdy, G., Van Der Zwaag, S., & Zurob, H. (2015). Overview of the current issues in austenite to ferrite transformation and the role of migrating interfaces therein for low alloyed

steels. In *Materials Science and Engineering R: Reports* (Vol. 92, pp. 1–38). Elsevier Ltd. https://doi.org/10.1016/j.mser.2015.03.001

Ha, H.-Y., Lee, T.-H., & Kim, S.-J. (2012). Role of nitrogen in the active–passive transition behavior of binary Fe–Cr alloy system. *Electrochimica Acta*, *80*, 432–439. https://doi.org/10.1016/j.electacta.2012.07.056

Han, Y., Liu, Z. H., Wu, C. B., Zhao, Y., Zu, G. Q., Zhu, W. W., & Ran, X. (2023). A short review on the role of alloying elements in duplex stainless steels. *Tungsten*, *5*(4), 419–439. https://doi.org/10.1007/s42864-022-00168-z

Javeria, U., & Kim, S. J. (2025). Investigation of hydrogen embrittlement in steel alloys: mechanism, factors, advanced methods and materials, applications, challenges, and future directions: A review. *Journal of Materials Research and Technology*. https://doi.org/10.1016/j.jmrt.2025.07.269

Kahar, Dr. S. D. (2017). Duplex Stainless Steels-An overview. *International Journal of Engineering Research and Applications*, *07*(04), 27–36. https://doi.org/10.9790/9622-0704042736

Kim, S.-C., Zhang, Z., Furuya, Y., Kang, C.-Y., Sung, J.-H., Ni, Q.-Q., Watanabe, Y., & Kim, I.-S. (n.d.). *Effect of Precipitation of-Phase and N Addition on the Mechanical Properties in 25Cr-7Ni-4Mo-2W Super Duplex Stainless Steel*.

Łabanowski, J., ̄wierczyńska, A., & Topolska, S. (2014). Effect of microstructure on mechanical properties and corrosion resistance of 2205 duplex stainless steel. *Polish Maritime Research*, *21*(4), 108–112. https://doi.org/10.2478/pomr-2014-0047

Lee, J. B. (2006). Effects of alloying elements, Cr, Mo and N on repassivation characteristics of stainless steels using the abrading electrode technique. *Materials Chemistry and Physics*, *99*(2–3), 224–234. https://doi.org/10.1016/j.matchemphys.2005.10.016

Levey, P. R., & van Bennekom, A. (1995a). A Mechanistic Study of the Effects of Nitrogen on the Corrosion Properties of Stainless Steels. *Corrosion*, *51*, 911–921. https://api.semanticscholar.org/CorpusID:97036791

Levey, P. R., & van Bennekom, A. (1995b). A Mechanistic Study of the Effects of Nitrogen on the Corrosion Properties of Stainless Steels. *Corrosion*, *51*(12), 911–921. https://doi.org/10.5006/1.3293567

Li, F., Liu, G., Liu, S., Zhu, Y., Dong, M., & Zhang, B. (2024). Effect of strain rate on the stress corrosion cracking of TP439 stainless steel in water vapor environment at 500 °C. *Surface Science and Technology*, *2*(1). https://doi.org/10.1007/s44251-024-00036-7

Li, J., Ma, Z., Xiao, X., Zhao, J., & Jiang, L. (2011). On the behavior of nitrogen in a low-Ni high-Mn super duplex stainless steel. *Materials and Design*, *32*(4), 2199–2205. https://doi.org/10.1016/j.matdes.2010.11.021

Liou, H. Y., Pan, Y. T., Hsieh, R. I., & Tsai, W. T. (2001). Effects of alloying elements on the mechanical properties and corrosion behaviors of 2205 duplex stainless steels. *Journal of Materials Engineering and Performance*, *10*(2), 231–241. https://doi.org/10.1361/105994901770345268

Liu, X., Zhang, X., Wu, J., Zhu, H., & Wu, Y. (2022). Mediating phase decomposition to avoid thermal aging embrittlement in a duplex stainless steel. *Materials Characterization*, *194*. https://doi.org/10.1016/j.matchar.2022.112411

Martin, M. L., Dadfarnia, M., Nagao, A., Wang, S., & Sofronis, P. (2019). Enumeration of the hydrogen-enhanced localized plasticity mechanism for hydrogen embrittlement in structural materials. In *Acta Materialia* (Vol. 165, pp. 734–750). Acta Materialia Inc. https://doi.org/10.1016/j.actamat.2018.12.014

Moverare, J. J., & Odé, M. (n.d.). *Influence of Elastic and Plastic Anisotropy on the Flow Behavior in a Duplex Stainless Steel*.

Newman, R. C., & Shahrabi, T. (1987). THE EFFECT OF ALLOYED NITROGEN OR DISSOLVED NITRATE IONS ON THE ANODIC BEHAVIOUR OF AUSTENITIC STAINLESS STEEL IN HYDROCHLORIC ACID. In *Corrosion Science* (Vol. 27, Issue 8).

Nilsson, J. O. (1992). Super duplex stainless steels. *Materials Science and Technology (United Kingdom)*, *8*(8), 685–700. https://doi.org/10.1179/mst.1992.8.8.685

Palit, G. C., Kain, V., & Gadiyar, H. S. (1993). Electrochemical Investigations of Pitting Corrosion in Nitrogen-Bearing Type 316LN Stainless Steel. *Corrosion*, *49*(12), 977–991. https://doi.org/10.5006/1.3316025

Papula, S., Anttila, S., Talonen, J., Sarikka, T., Virkkunen, I., & Hänninen, H. (2016). Strain hardening of cold-rolled lean-alloyed metastable ferritic-austenitic stainless steels. *Materials Science and Engineering: A*, *677*, 11–19. https://doi.org/10.1016/j.msea.2016.09.038

Park, C.-J. (2002). Effects of aging at 475° C on corrosion properties of tungsten-containing duplex stainless steels. *Corrosion Science - CORROS SCI*, *44*. https://doi.org/10.1016/S0010-938X(02)00079-3

Paulraj, P., & Garg, R. (2015). Effect of Intermetallic Phases on Corrosion Behavior and Mechanical Properties of Duplex Stainless Steel and Super-Duplex Stainless Steel. *Advances in Science and Technology Research Journal*, *9*(27), 87–105. https://doi.org/10.12913/22998624/59090

Raina, A., Deshpande, V. S., & Fleck, N. A. (2017). *Analysis of thermal desorption of hydrogen in metallic alloys*.

Ravindranath, K., & Malhotra, S. N. (1995). THE INFLUENCE OF AGING ON THE INTERGRANULAR CORROSION OF 22 CHROMIUM-5 NICKEL DUPLEX STAINLESS STEEL. In *Corrosion Science* (Vol. 37, Issue 1).

Sobola, D., & Dallaev, R. (2024). Exploring Hydrogen Embrittlement: Mechanisms, Consequences, and Advances in Metal Science. In *Energies* (Vol. 17, Issue 12). Multidisciplinary Digital Publishing Institute (MDPI). https://doi.org/10.3390/en17122972

Sun, B., Wang, D., Lu, X., Wan, D., Ponge, D., & Zhang, X. (2021). Current Challenges and Opportunities Toward Understanding Hydrogen Embrittlement Mechanisms in Advanced High-Strength Steels: A Review. In *Acta Metallurgica Sinica (English Letters)* (Vol. 34, Issue 6, pp. 741–754). Chinese Society of Metals. https://doi.org/10.1007/s40195-021-01233-1

Vargel, C. (2020). Preface. In C. Vargel (Ed.), *Corrosion of Aluminium (Second Edition)* (Second Edition, pp. xxxix–xl). Elsevier. https://doi.org/https://doi.org/10.1016/B978-0-08-099925-8.05001-8

Zakroczymski, T., Glowacka, A., & Swiatnicki, W. (2005). Effect of hydrogen concentration on the embrittlement of a duplex stainless steel. *Corrosion Science*, *47*(6), 1403–1414. https://doi.org/10.1016/j.corsci.2004.07.036

Zhang, D., Liu, A., Yin, B., & Wen, P. (2022). Additive manufacturing of duplex stainless steels - A critical review. *Journal of Manufacturing Processes*, *73*(August 2021), 496–517. https://doi.org/10.1016/j.jmapro.2021.11.036